Testing the parton evolution with the use of two-body final states

S.P. Baranov

P.N. Lebedev Physics Institute, 119991 Moscow, Russia

H. Jung

Deutsches Elektronen-Synchrotron, Notkestrasse 85, Hamburg, Germany

A.V. Lipatov

Skobeltsyn Institute of Nuclear Physics,

Lomonosov Moscow State University, 119991 Moscow, Russia and

Joint Institute for Nuclear Research,

Dubna 141980, Moscow region, Russia

M.A. Malyshev

Skobeltsyn Institute of Nuclear Physics,

Lomonosov Moscow State University, 119991 Moscow, Russia

Abstract

We consider the production of $b\bar{b}$ quarks and Drell-Yan lepton pairs at LHC conditions focusing attention on the total transverse momentum of the produced pair and on the azimuthal angle between the momenta of the outgoing particles. Plotting the corresponding distributions in bins of the final state invariant mass, one can reconstruct the full map of the transverse momentum dependent parton densities in a proton. We give examples of how can these distributions can look like at the LHC energies.

1

Experiments of new generation running at the LHC yield plenty of high precision data. In order to properly interpret these data we need that the parton distribution functions to be known with adequately good accuracy. This, in turn, rises question on a detailed measurement of parton distributions. In this note we focus attention on two important kinematic observables which enable us to reconstruct the full map of the transverse momentum dependent (TMD), or unintegrated, parton densities. We address our consideration to the LHC conditions (pp collisions at $\sqrt{s} = 7$ TeV), for which we give a number of illustrations.

The evolution of TMD gluon densities can be explored with the production of $b\bar{b}$ pairs. At the LHC energies, this process is dominated by the direct leading-order (LO) off-shell gluon-gluon fusion subprocess

$$g^*(k_1) + g^*(k_2) \to b(p_1) + \bar{b}(p_2), \tag{1}$$

while the contribution from the quark-antiquark annihilation is of almost no importance because of comparatively low quark densities. The four-momenta of corresponding particles are given in the parentheses. The present calculation of the process (1) is fully identical to that performed previously [1]. The evolution of TMD quark densities can be explored with the production of Drell-Yan lepton pairs. This process is dominated by the off-shell quark-antiquark ahhihilation subprocess

$$q^*(k_1) + \bar{q}^*(k_2) \to l^+(p_1) + l^-(p_2), \tag{2}$$

where q includes valence and sea quarks and $\bar{q}$ stands for sea anti-quarks. The present calculation of the process (2) is fully identical to that from [2]. We do not consider here higher-order corrections $q + \bar{q} \to l^+ + l^- + g$ since they are already taken into account in the k_T-factorization approach [3–5] as a part of the evolution of TMD quark densities.

The final states of the processes (1) and (2) are represented by two-body systems with fully reconstructable kinematics where the transverse momentum p_T of the $b\bar{b}$ or lepton pair measures the net transverse momentum of the initial gluons or quarks, the invariant mass of the pair measures the product of longitudinal momentum fractions, $M^2 = x_1 x_2 s$, and the rapidity of the pairs measures the ratio of the momentum fractions, $y = (1/2) \ln(x_1/x_2)$. A useful complementary observable is the difference between the azimuthal angles of produced particles $\Delta\phi$. In the LO of collinear QCD factorization, the p_T and $\Delta\phi$ distributions degenerate into delta functions at $p_T = 0$ and $\Delta\phi = 0$, and the continuous spectra can

only be obtained by including higher-order corrections. In the k_T-factorization approach, these radiative corrections are automatically taken into account in the form of TMD parton densities. Comparing the p_T and $\Delta\phi$ spectra at varying gluon momentum fraction x we watch the evolution of parton distributions.

To simulate the $b\bar{b}$ pair production we used the latest JH'2013 parametrization [6] for the TMD gluon densities in a proton. The input parameters of this gluon distribution were fitted to describe the proton structure function F_2. To simulate the production of Drell-Yan lepton pairs we applied complementary TMD valence quark distributions from the same set [6]. The necessary TMD sea quark densities are calculated from the gluon ones in the approximation where the sea quarks occur in the last gluon-to-quark splitting [7].

The results of our calculations are displayed in Figs. 1 — 7. Shown in Figs. 1 and 2 are the spectra of $b\bar{b}$ pair and dilepton transverse momentum p_T and the azimuthal angle $\Delta\phi$ plotted for several different intervals of their invariant mass M. Here, to make the changes in shape easier recognizable, we show the normalized differential cross sections. We see that with increasing M the maximum in the p_T spectrum shifts gradually to higher values, and the whole distribution becomes more flat. The $\Delta\phi$ distribution moves towards $\Delta\phi \simeq \pi$, that is due to the inequality $M \gg p_T$. The latter becomes even stronger at high M (see Fig. 3). As one can see from Fig. 2, quark distributions follow the same trend as gluon densities.

The observed behaviour of calculated p_T and $\Delta\phi$ distributions is related to the different regions of x and/or parton transverse momenta probed in the considered M bins. In fact, with increasing of M, the achieved x values shifted towards unity, irrespectively on the rapidities of final-state particles, as it is demonstrated in Figs. 4 and 5. The latter results to decreasing of average parton transverse momentum generated in the non-collinear parton evolution. At the highest M bin, this average parton transverse momentum becomes small compared to the hard scale (which is order of M), so that the collinear kinematics of the partonic subprocesses are reproduced.

Besides the restrictions on the invariant mass, the special kinematical cuts on the final state give us further possibilities to achive the wanted region of x and/or partonic transverse momenta. It is illustrated in Figs. 6 and 7, where we plot the normalized differential cross sections of the considered subprocesses calculated as a functions of x and $\mathbf{k}_T^2$ (the longitudinal momentum fraction and transverse momentum of one of the colliding partons) with the additional cuts applied to the rapidity y of the final state quark or lepton pair. As an

example, we used $y < 1$ and $3 < y < 4$. We show that under these cuts one can probe different x and/or $\mathbf{k}_T^2$ regions and extract an information on the TMD parton distributions at the scale given by M. Note that the different $\mathbf{k}_T^2$ regions can be achieved under additional restrictions on the quark or lepton pair transverse momentum p_T and/or azimuthal angle $\Delta\phi$.

Thus, we conclude that one can map the evolution of parton distributions at the scale M from high values of proton longitudinal momentum fraction x to low ones by applying different cuts on the final states. This is important to further precise determination of the TMD quark and gluon densites in a proton from the LHC data.

[1] H. Jung, M. Krämer, A.V. Lipatov, N.P. Zotov, Phys. Rev. D **85**, 034035 (2012).

[2] S.P. Baranov, A.V. Lipatov, N.P. Zotov, Phys. Rev. D **89**, 094025 (2014).

[3] L.V. Gribov, E.M. Levin, M.G. Ryskin, Phys. Rep. **100**, 1 (1983);
   E.M. Levin, M.G. Ryskin, Phys. Rep. **189**, 268 (1990).

[4] S. Catani, M. Ciafaloni, F. Hautmann, Phys. Lett. B **242**, 97 (1990); Nucl. Phys. B **366**, 135 (1991).

[5] J.C. Collins, R.K. Ellis, Nucl. Phys. B **360**, 3 (1991).

[6] H. Jung, F. Hautmann, Nucl. Phys. B **883**, 1 (2014).

[7] F. Hautmann, M. Hentschinski, H. Jung, arXiv:1205.1759 [hep-ph].
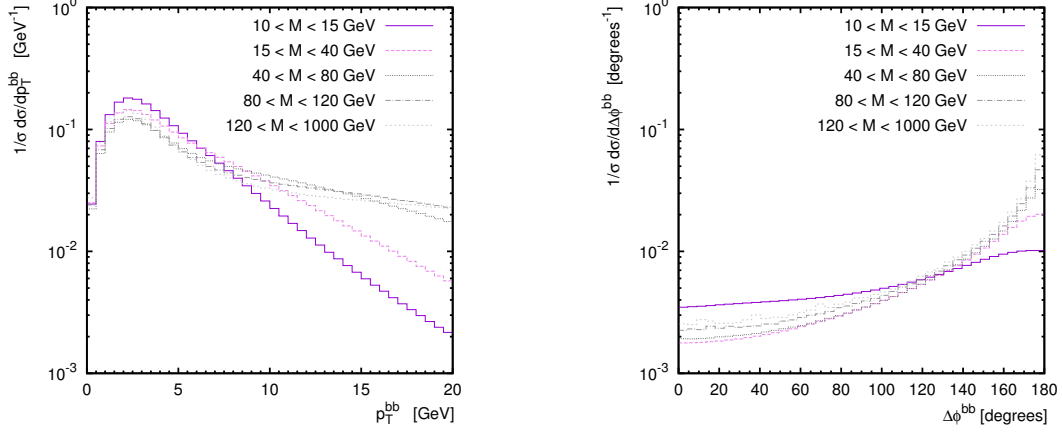
FIG. 1. Spectra of the $b\bar{b}$ pair transverse momentum p_T and the azimuthal angle between the beauty quarks $\Delta\phi$ for several different intervals of the $b\bar{b}$ invariant mass M.
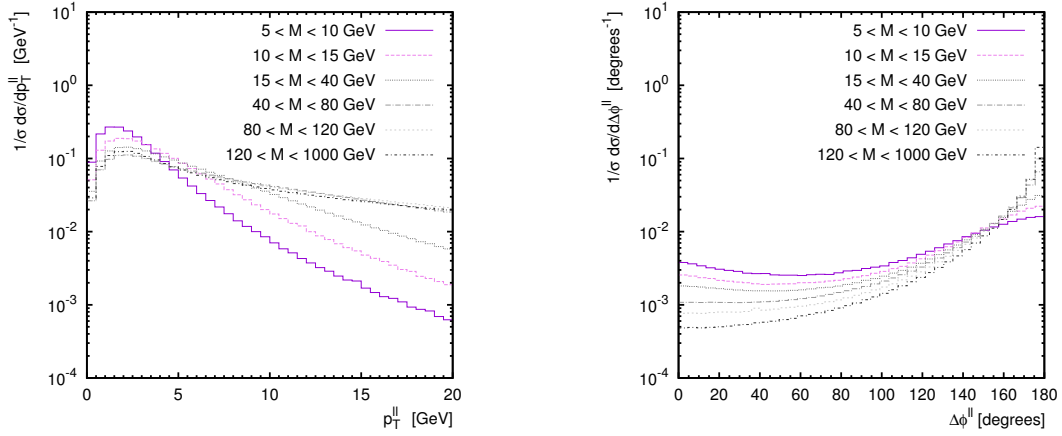

FIG. 2. Spectra of the Drell-Yan lepton pair transverse momentum p_T and the azimuthal angle between the produced leptons $\Delta\phi$ for several different intervals of the dilepton invariant mass M.
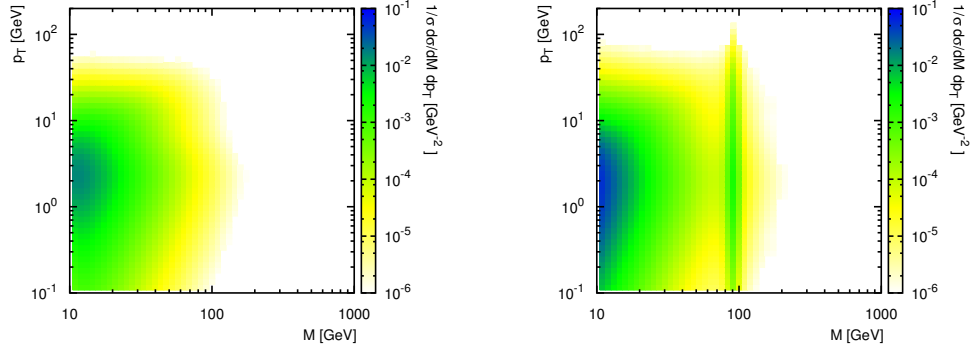
FIG. 3. Double differential cross sections of the $b\bar{b}$ (left panel) and Drell-Yan lepton pair production (right panel) as a functions of invariant mass M and p_T of the produced pair.
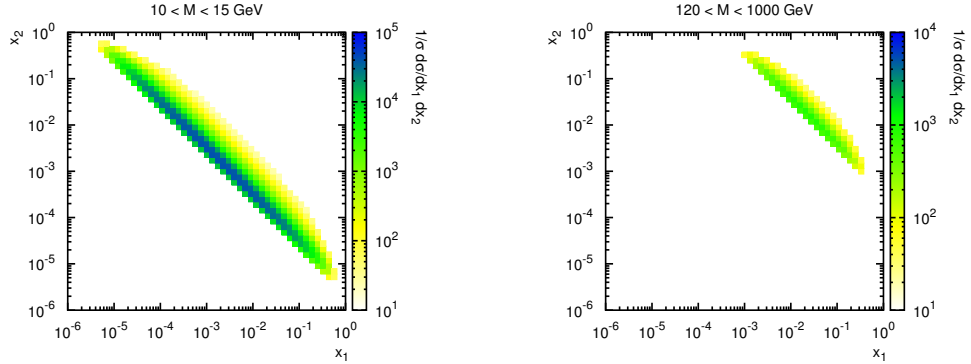

FIG. 4. Double differential cross sections of the $b\bar{b}$ pair production as a functions of x_1 and x_2 for several different intervals of the $b\bar{b}$ invariant mass M.
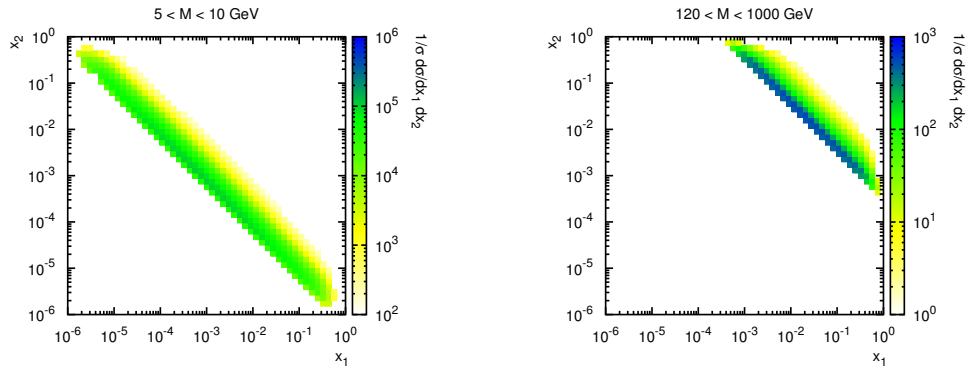

FIG. 5. Double differential cross sections of the Drell-Yan lepton pair production as a functions of x_1 and x_2 for several different intervals of the dilepton invariant mass M.
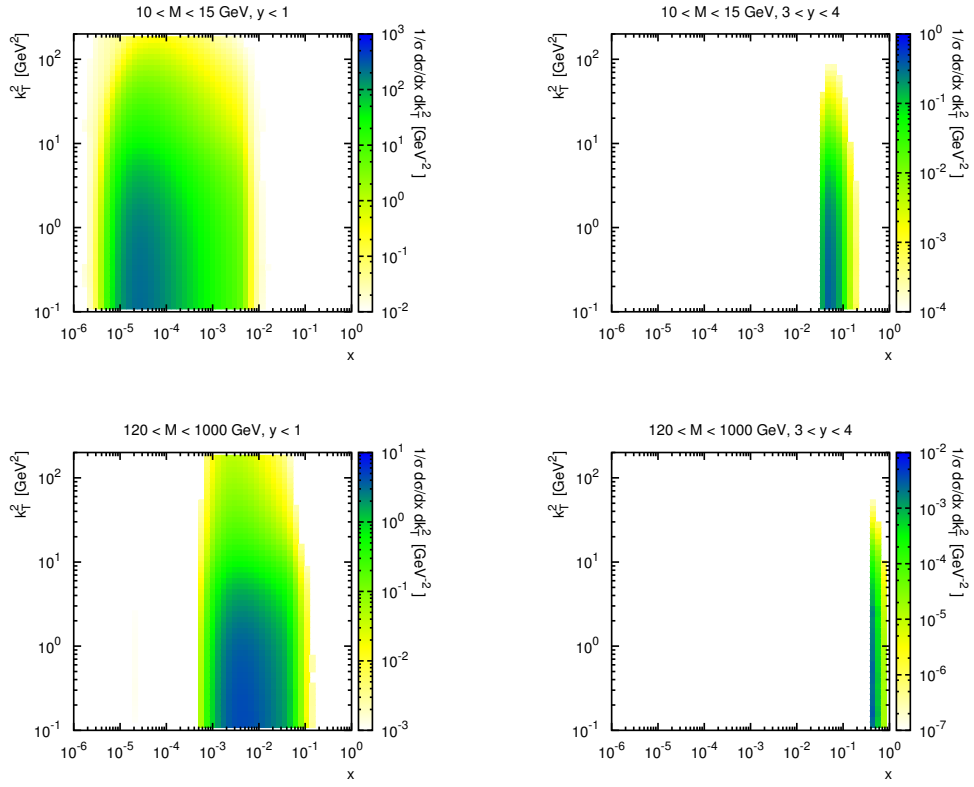
FIG. 6. Double differential spectra of the $b\bar{b}$ pair production as a function of x and $\mathbf{k}_T^2$ for several different intervals of the $b\bar{b}$ invariant mass M and rapidity y.
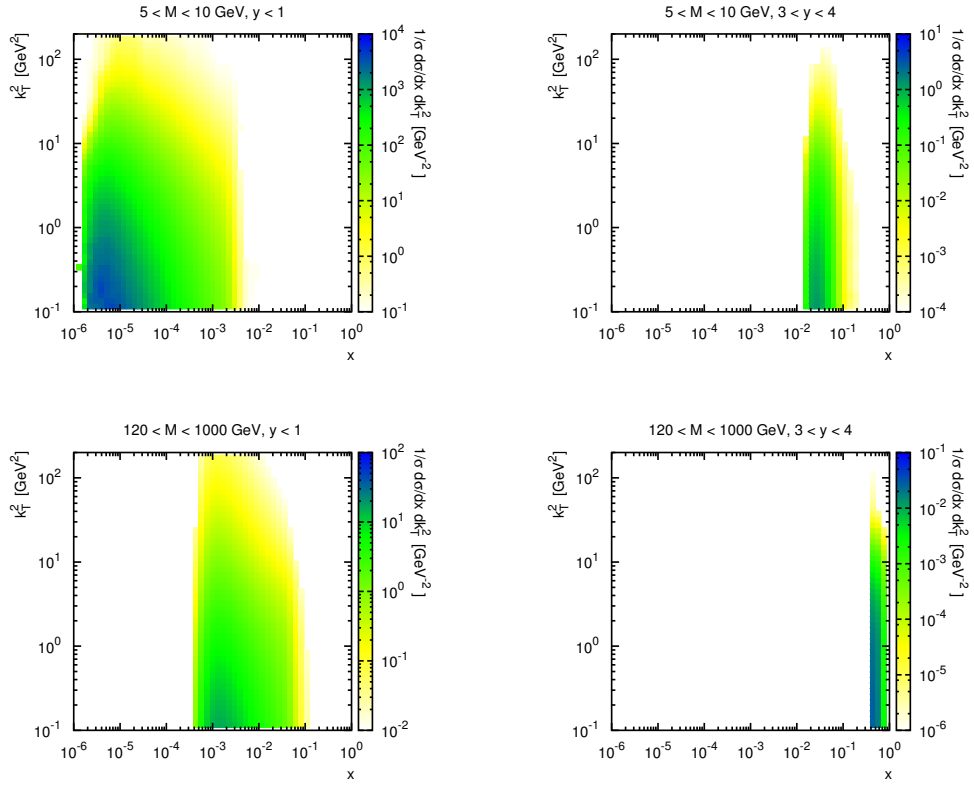
FIG. 7. Double differential spectra of the Drell-Yan pair production as a function of x and $\mathbf{k}_T^2$ for several different intervals of the dilepton invariant mass M and rapidity y.